



Magnetic Flux Reconnection in Flaring Active Regions with Sustained Gamma-Ray Emission

S. W. Kahler¹ , E. W. Cliver² , and M. Kazachenko³ 

¹ Air Force Research Laboratory, Space Vehicles Directorate, 3550 Aberdeen Ave., Kirtland AFB, NM 87117, USA; stephen.kahler@us.af.mil

² National Solar Observatory, Boulder, CO, USA

³ Space Sciences Laboratory, University of California, Berkeley, CA 94720, USA

Received 2018 September 19; revised 2018 October 17; accepted 2018 October 17; published 2018 November 26

Abstract

Characteristics of sustained >100 MeV γ -ray emission (SGRE) events observed by the Large Area Telescope on *Fermi* were recently reported by Share et al. Their spectra are consistent with the decay of pions produced by >300 MeV protons and appear spectrally and spatially distinct from preceding associated flares. The source(s) of the sustained production of the >300 MeV protons is uncertain, but acceleration in coronal/interplanetary shock waves driven by coronal mass ejections, followed by a return of the protons back to the Sun, is favored. This scenario requires proton transport through converging magnetic fields behind the shock, which might result in considerable reflection of the protons back into space, and 1 au observations of the associated solar energetic proton (SEP) events do not always include a population of $E > 300$ MeV protons. Alternative source candidates that involve trapping or continued acceleration of SEPs in coronal loops have been considered. The energy release rates from magnetic reconnection in flaring active regions (ARs) have been measured with a new technique, and in this work we compare those measured flux reconnection rates with emission profiles in 11 SGRE events. In general, the magnetic reconnection event is nearly or completely finished before the bulk of the γ -ray emission, which argues against scenarios of continued proton acceleration in the flaring ARs.

Key words: acceleration of particles – magnetic reconnection – Sun: coronal mass ejections (CMEs) – Sun: flares – Sun: particle emission – Sun: X-rays, gamma rays

1. Introduction

Since its launch in 2008 June the *Fermi* Large Area Telescope (LAT, Atwood et al. 2009) has greatly enhanced our ability to detect high-energy ($E > 100$ MeV) γ -ray flares on the Sun. These events result from decays of neutral pions (Ackermann et al. 2014) produced in interactions of $E \gtrsim 300$ MeV protons with ambient protons or of $E \gtrsim 200$ MeV protons with ambient alphas (Murphy et al. 1987) in the solar atmosphere. While $E > 100$ MeV γ -ray emission might have been expected from flare impulsive phases, observations of emission extending for up to 20 hr after the impulsive phases, now known as sustained γ -ray emission (SGRE, Ackermann et al. 2014; Share et al. 2018), has been a continuing challenge to our understanding of energetic particle acceleration and transport.

SGRE events have been observed with various γ -ray experiments (Hudson & Ryan 1995; Kuznetsov et al. 2014) since the first event on 1982 June 3 (Forrest et al. 1985). The occurrence of a type II radio burst and fast coronal mass ejection (CME) suggested to Ramaty et al. (1987) that a precipitation back to the Sun of $<10\%$ of the solar energetic protons (SEPs) produced in the second phase shock acceleration could produce the 1982 June 3 SGRE event. The first SGRE with a duration of several hours (1991 June 11; 50–2000 MeV γ -rays for ~ 8 hr) was reported by Kanbach et al. (1993) based on observations with the highly sensitive Energetic Gamma Ray Experiment Telescope on the Compton Gamma Ray Observatory. In response to such observations, the precipitating particle interpretation was then generally rejected in favor of a coronal magnetic loop-trapping mechanism (Mandzhavidze & Ramaty 1992), the question then being whether the particles were impulsively or gradually accelerated

in the trapping loops (Ramaty & Mandzhavidze 1996). Ryan (2000) reviewed three possible models for SGRE events. The first was trapping of particles in static coronal loops, where a continuous acceleration process in the loops was favored over passive trapping of an impulsive phase injection, as Hudson & Ryan (1995) had previously concluded. A prime difficulty with the passive trapping concept was particle loss from the loop due to curvature and gradient drifts. The second was electric field acceleration in reconnecting current sheets behind the associated fast CME. The third, and least favored, was precipitation from the CME-driven shock.

The first SGRE event associated with a flare behind the limb was observed on 1989 September 29 with the Gamma Ray Spectrometer on the *Solar Maximum Mission* (SMM) spacecraft. Vestrand & Forrest (1993) found the SGRE region in that event to extend over 30° on the solar surface and suggested either particles diffusing from flare loops or precipitating from a coronal shock as the explanation for the large extent. Cliver et al. (1993) noted that the 1989 September 29 flare was associated with the largest high-energy SEP event at Earth since 1956 (with protons detected at ~ 20 GeV). They argued that for both the protons observed in space and those interacting at the Sun to produce SGREs, the required “transport” of the protons to the front side of the Sun was accomplished by widespread acceleration at a CME-driven shock.

The observation of three *Fermi*/LAT SGRE events, on 2013 October 11, 2014 January 6, and 2014 September 1, associated with flares occulted behind the limb (Pesce-Rollins et al. 2015; Ackermann et al. 2017) have provided more guidance on the origins of these events. All were associated with very fast CMEs and SEP events at 1 au, suggesting the precipitation model. Plotnikov et al. (2017) modeled the three events with a

potential field source surface and an MHD model to determine the development of magnetic connectivities of CME-driven shocks to the photosphere. They found that SEPs from the shocks could sustain the SGRE events on the visible disk as well as escape to interplanetary space. Kocharov et al. (2015) modeled the production of SEPs in a spherical shock propagating through a turbulent radial ray surrounded by a weakly turbulent region that allows for SEP escape to Earth and back to the Sun. The Sun-propagating particle component, which produces the SGRE nuclear interactions, may undergo stochastic re-acceleration in the enhanced turbulence behind the shock.

A somewhat more extensive approach was taken by Afanasiev et al. (2018) to model the disk SGRE events of 2012 January 23 and May 17 (a ground level enhancement (GLE)) by combining a coronal shock model with a Down-Stream Propagation (DSP) model, which included diffusive downstream particle transport. They also found particle precipitation a viable option for SGRE events, supporting the conclusions of Pesce-Rollins et al. (2015) and Ackermann et al. (2017). The variation in shock magnetic connection to the photosphere could account for the possible east–west drift observed in the 2012 March 7 SGRE event (Ajello et al. 2014). Recently, Share et al. (2018) carried out a study of 30 *Fermi*/LAT $E > 100$ MeV SGRE events and related solar observations from 2008 June to 2016 December. Those authors also favor a precipitation model for the SGRE events, following an injection of sub-MeV to MeV protons as a seed population from the flare into the CME-driven shock.

Other authors have doubts about the precipitation model. Ryan & de Nolfo (2018) invoke large-scale $\sim 1 R_{\odot}$ quasi-static loops as the source regions of two SGREs on 2012 March 7, specifically excluding CME roles in those events. They do not specify the spatial or temporal relationships between CME magnetic fields and those of the quasi-static loops or whether the energetic particles are passively trapped or actively accelerated in the loops. Hudson (2018) has proposed that SEP acceleration must occur in both open and closed loop field lines and suggests a lasso model, in which a very distended loop structure, possibly extending to several R_{\odot} , retracts to transport energetic particles by advection back to denser regions. Such loops might be observed as post-CME inward flows (Sheeley & Wang 2014) due to interchange reconnection between closed loops of the CME and open field lines of an adjacent coronal hole, but a CME-driven shock may not leave particles on the closed field lines of the trailing CME itself. The “Rosetta Stone” event for Hudson’s proposed scenario for SGREs was the LAT flare of 2014 September 1. The time profile and spectral evolution of this event has similarities to the γ -ray flare on 1991 June 15 analyzed by Akimov et al. (1996). In both the Hudson (2018) and Akimov et al. (1996) studies, sustained high-energy γ -ray emission is linked to post-eruption or post-impulsive-phase activity, with the emphasis in the Akimov et al. (1996) study on delayed reconnection/acceleration and that of Hudson focused on particle trapping, although the collapsing trap would be expected to further accelerate the enclosed particles.

Kuznetsov et al. (2014) examined four pion-decay flare events with the *CORONAS-F* SONG instrument. They found that $E > 300$ MeV protons were produced beginning in the impulsive phase and at the same time as the solar release time (SRT) of GLE particles observed in ground-based neutron

monitors. They further found good correlations between $E > 60$ MeV emission and both active region (AR) magnetic flux changes and derivatives of the profiles of soft X-ray emission. Kuznetsov et al. (2014) did not distinguish between impulsive and sustained GRE components, but they make clear that in their events most of the $E > 300$ MeV proton production occurs early in the flare process and exceeds 10 minutes. This would be consistent with a flare source for the entire durations of their events.

Klein et al. (2018) claim significant correlations between peak fluxes of the SGRE events and the preceding soft X-ray flares. They also find a general trend for longer-duration SGRE events to have longer-duration soft X-ray events, indicating a continued coronal energy release in those events. They argue that particles injected from a shock back to the Sun in a radial magnetic field will undergo reflections that allow at most only about 1% of the initial particles to precipitate. Another challenge is that in the well-connected W47° flare of 2011 March 7 the SRT from L1 observations was 20 minutes later than the SGRE onset and the peak energy at L1 did not exceed 80 MeV, below the threshold for pion production. Hudson (2018) also raised similar objections against the precipitation model based on SEP reflections in coronal magnetic fields and on insufficient energies of SEP events. These two points are directly addressed by Afanasiev et al. (2018), whose DSP transport model of particle flow to the Sun is based on a Monte Carlo calculation of particle scattering in a turbulent field including advection and adiabatic deceleration. The ideal radial magnetic field invoked by Kocharov et al. (2015), Klein et al. (2018), and Hudson (2018) is not used in realistic SEP transport models. Because of variations of shock acceleration efficiency from one flux tube to another, Afanasiev et al. (2018) pointed out that an SGRE event may well occur without a clear increase observed at 1 au of energies required for pion production.

A related basic question is whether flares play a significant role in the production of gradual SEP events observed at 1 au (Kahler et al. 2017; Cliver et al. 2018). The publication of a database of 3137 flare reconnection fluxes (RibbonDB; Kazachenko et al. 2017), i.e., the amount of unsigned photospheric magnetic flux swept out by flare ribbons, has allowed us (Kahler et al. 2017) to compare 15 peak 25 MeV SEP event intensities with the reconnection fluxes of 128 well-connected (W20°–W45°) flares. The SEP peak intensities did not show a correlation with reconnection fluxes. However, Kazachenko et al. (2017) found a good correlation between logs of *GOES* peak soft X-ray flux and logs of reconnection flux ($CC = 0.66$) and of ribbon area ($CC = 0.68$). With a small (51 events) subset of the Kazachenko et al. (2017) events and using their own measurements, Toriumi et al. (2017) found good correlations of *GOES* soft X-ray flare FWHM and decay time with reconnection flux and ribbon area. Although they found lower CCs for the flare peak X-ray fluxes and reconnection fluxes and ribbon areas, it is clear that there is a close connection between timescales and intensities of *GOES* flare X-ray events and reconnection parameters. However, the reconnection rates in each flare ribbon give us direct measures of the energy release in the AR magnetic fields that would be available for the acceleration of the $E > 300$ MeV protons needed to sustain the SGRE events.

Does the production of SGRE events occur in quasi-static large-scale coronal loops (Ryan & de Nolfo 2018) or in the

Table 1
Magnetic Flux Reconnections in SGREs

Date and Event #	Location	GOES X-Ray Class, Peak	Reconnect P, N Peak	Reconnect P, N End	SGRE Total Interval, UT	10^{28} Protons >500 MeV
20110602 2 (217)	S19E25	C3.7 07:46	07:41 P 07:41 N	07:56 07:56	08:10–12:00	0.03 ± 0.02
20110804 4 (277)	N19W36	M9.3 03:57	03:45 P 03:52 N	04:00 04:00	04:20–07:10	1.2 ± 0.3
20110906 6 (304)	N14W18	X2.1 22:20	22:18 P 22:18 N	22:24 22:24	22:21–23:20	2.2 ± 0.4
20110907 7 (306)	N14W28	X1.8 22:38	22:35 P 22:35 N	22:45 22:45	22:45–01:10	0.2 ± 0.1
20120123 9 (512)	N28W21	M8.7 03:59	03:40 P 03:47 N	04:30 04:16	04:20–12:00	3.0 ± 0.6
20120307 12 (540)	N17E29	X5.4 00:24	00:06 P 00:06 N	00:36 00:27	00:28–01:24 (A)	40 ± 15
20120307 12 (541)	N17E20	X1.3 01:14	01:07 P 01:07 N	01:22 01:21	02:00–20:01 (B)	131 ± 15
20120309 13 (545)	N17E01	M6.3 03:53	03:25 P 03:39 N	03:54 03:59	04:30–10:30	1.5 ± 0.6
20130411 20 (1139)	N09E12	M6.5 07:16	07:00 P 07:02 N	07:17 07:17	07:10–07:30	0.74 ± 0.3
20131028 27 (1488)	S08E26	M4.4 15:15	15:09 P 15:07 N	15:15 15:12	15:20–17:00	0.04 ± 0.02
20150621 30 (2817)	N13E14	M2.6 02:36	02:08 P 02:06 N	02:40 02:51	02:20–14:00	1.4 ± 0.7

retraction of large-scale closed fields (Hudson 2018)? Both scenarios require the $E > 300$ MeV particle population to be accelerated and/or trapped in the inferred loops for periods of hours. A similar SGRE candidate for particle acceleration and precipitation not due to the CME-driven shock would be magnetic reconnection in AR flare loops formed behind the CME.

In this work we compare time profiles of the AR reconnection ribbon fluxes measured at 1600 \AA with the times of the associated SGRE events from the Share et al. (2018) study to determine whether the magnetic reconnection can provide a viable source of energy for the production of $E > 300$ MeV protons leading to the SGRE events through pion production.

2. Data Analysis

2.1. Event Selection and Criteria

A summary of SGRE events from the first four years (2008–2012) of LAT observations (Ackermann et al. 2014) was followed by a recent work by Share et al. (2018) listing and discussing properties of 30 SGRE events observed through 2015. Of the 30 SGREs in Table 1 of Share et al. (2018), we select for comparison all those with GOES X-ray flares located within 45° of the central meridian, which are included in the Kazachenko et al. (2017) database of flare ribbons. The event dates are listed in the first column of Table 1, along with the SGRE Table 1 and RibbonDB entry numbers. The flare locations are those from the Heliophysics Event Catalog maintained by the INAF-Trieste Astronomical Observatory and listed in the database. Our locations in Table 1 agree to within 3° – 5° with those of Table 1 of Share et al. (2018), except for our 20110804 location of N19W36 versus N19W46 of their Table 1. The GOES 1–8 \AA X-ray flare class and peak time are given in Column 3. Our X1.3 flare class for the second part of 20120307 disagrees with their flare listing of M3, which might

be appropriate if the tail of the preceding X5.4 flare is subtracted (Klein et al. 2018). That is event # 12 of Table 1 of Share et al. (2018), which consists of two flares in the same AR separated by slightly more than 1 hr (Ajello et al. 2014).

We examined the magnetic flux reconnection profiles calculated in units of $10^{18} \text{ Mx s}^{-1}$ separately for the positive and negative flare ribbons for all 11 events of Table 1. Figure 1 shows an example of the SGRE of 20110804. The right panel shows the reconnection rates of each ribbon and the cumulative reconnection flux in units of 10^{21} Mx . The left panel shows the ribbon mask over the radial field B_r , and the middle panel indicates the temporal development with a color-coded scale. Two further examples of SGRE events of Table 1 (#12, 20120307 (event A) and #20, 20130411) are shown in the bottom two rows of Figure 7 of Kazachenko et al. (2017). They are in the same format as our Figure 1, except that the reconnection rates are not included in the right panels.

Figure 2 shows only the reconnection flux and rate profiles for three additional events, on 2011 June 2, 2011 September 7, and 2015 June 21. The first and third events show complex reconnection profiles, while the middle one is a fairly simple profile. The reconnection profiles were examined for each event to determine the peaks and effective end times, defined as the times after which rates were $\leq 10^{18} \text{ Mx s}^{-1}$ for each ribbon. In all cases the reconnection peak times, as well as the 100–300 keV hard X-ray peaks shown in the plots of Share et al. (2018), preceded the peak times of the associated 1–8 \AA flare fluxes. This result is consistent with the suggestion (Kazachenko et al. 2017) of a correlation between peak reconnection flux rate and peak hard X-ray flux and also with earlier case studies (e.g., Qiu et al. 2004).

We show in Figure 3 the time lines for each SGRE event, where the reconnection times are the intervals from the earlier ribbon peak time to the later ribbon end time. The SGRE time intervals are the SGRE Total times from Table C2 of Share et al. (2018). The basic result is that most SGRE events

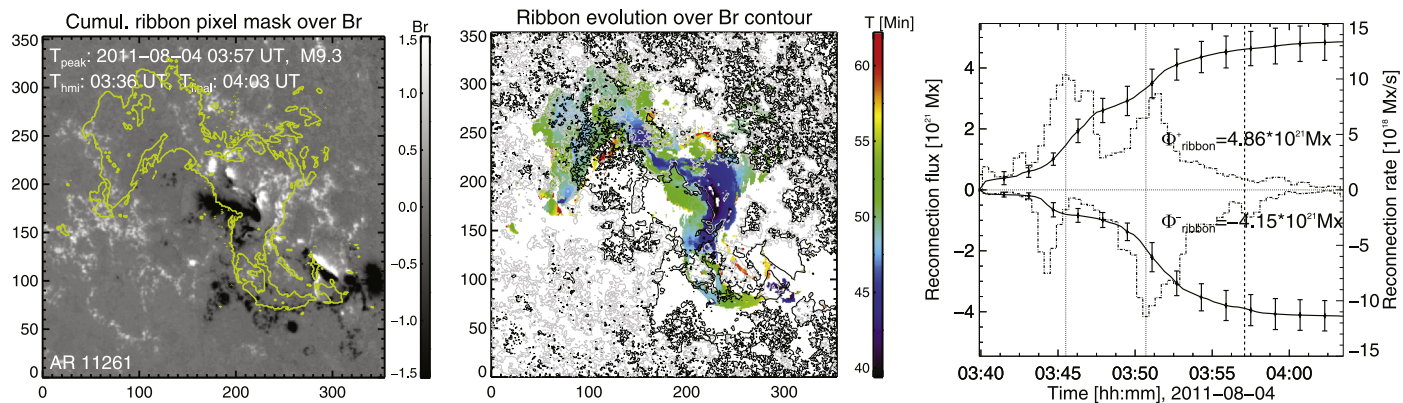


Figure 1. SGRE of 2011 August 4. Left: Heliospheric and Magnetic Imager (HMI) photospheric magnetogram B_r with the contours of the cumulative AIA 1600 Å flare ribbons at the flare end time overplotted. The times in the top-left corner are the GOES peak X-ray flux time (peak), time of HMI B_r observation (thmi), and the flare end time (tfinal). Middle: temporal and spatial evolution of the UV flare ribbons $M(x, y, tfinal)$ with each pixel colored by the time of its initial brightening. Right: time profiles of the total reconnection flux in units of Mx integrated in the positive and negative polarities, respectively (left scale). The errorbars in the reconnection flux indicate the range of uncertainty from the ribbon area identification. The reconnection rates are shown in steps of $Mx s^{-1}$ (right scale). Vertical dotted lines indicate peak reconnection times for each ribbon. The vertical dashed line marks the GOES peak X-ray flux time. Φ^+ and Φ^- ribbons indicate positive and negative reconnection fluxes at the tfinal end of the sequence.

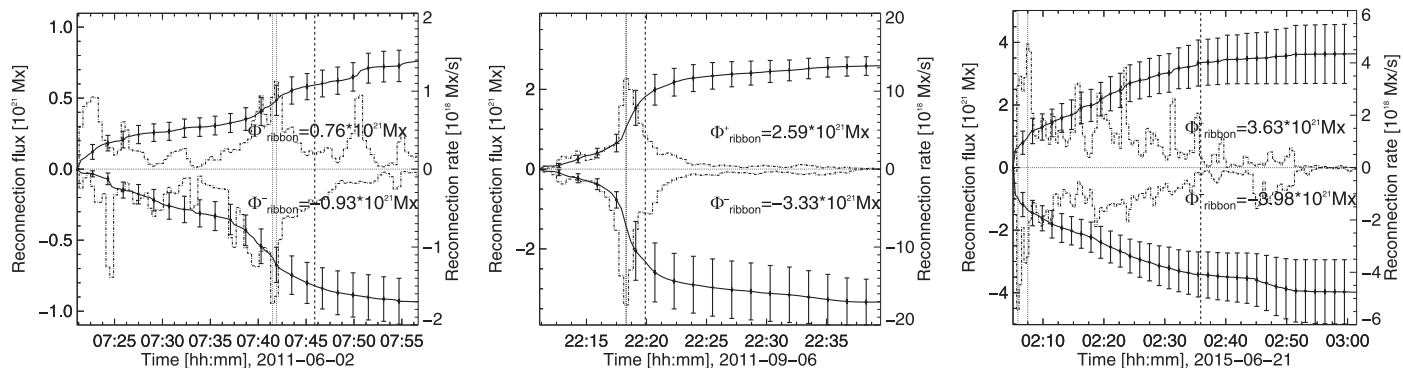


Figure 2. Reconnection flux and rate plots of three SGREs of Table 1. Events left to right: 2011 June 2; 2011 September 6; 2015 June 21. Each plot shows the cumulative reconnection flux (left scale) of the positive (top) and negative (bottom) magnetic regions. The reconnection rates of each polarity are shown with the right scale. Vertical dashed lines indicate the times of GOES X-ray flux peak times, and dotted lines are times of maximum reconnection rate in each magnetic polarity.

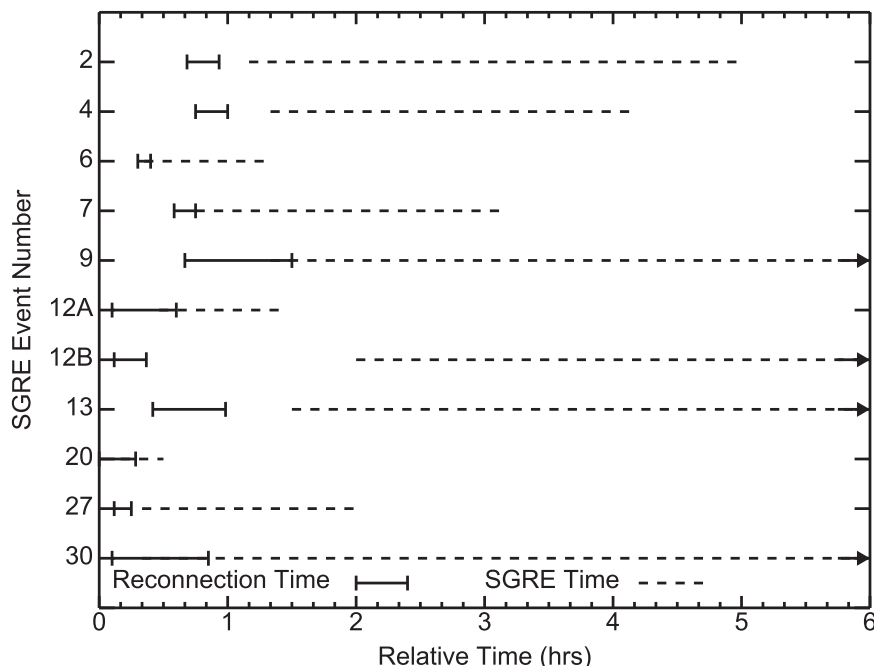


Figure 3. Flare reconnection intervals from peak to end compared with the times of associated SGREs. The 11 events of Table 1 are shown with times beginning at the hours of reconnection event peaks taken as 0. Arrows on the SGRE times indicate longer than 6 hr.

continue for hours after the effective terminations of the 1600 Å flare-ribbon reconnections. As Share et al. (2018) show, this is also the case for the SGRE events and the 100–300 keV hard X-ray bursts. Only events 7, 12A, and 20 have durations less than an hour and might therefore be the result of particle acceleration during the AR magnetic flux reconnection.

3. Discussion

There are two primary candidate concepts for the production of SGRE events, the first being precipitation back to the Sun of SEPs accelerated in CME-driven shocks. The observational motivation has been the occurrence of SGRE events associated with flares behind the solar limb. Those events require that SEPs interact with ions in the solar atmosphere—the photosphere or chromosphere—to produce the pions leading to SGRE over broad longitude and latitude regions well removed from the flaring AR. That concept is consistent with our observation that there is essentially no continued energy release through magnetic reconnection in the flare AR and that models (Plotnikov et al. 2017; Afanasiev et al. 2018) have shown the viability of SEP precipitation from shocks back through the stronger magnetic fields of the solar corona. With only a sparse rain of $E > 100$ MeV protons to produce the SGRE, we may not expect to see a sufficient precipitation of low energy SEPs to produce coronal or chromospheric heating with observable consequences.

Our results (Figure 3) rule out the scenario of Ryan (2000) of particle acceleration in the reconnection electric fields behind the CME because the required AR magnetic arcade formation is terminated well before the extended periods of the SGREs. In addition, such reconnection electric fields could not account for spatially extended SGREs such as those associated with behind-the-limb flares. The observations do not directly rule out possibilities of the large, long-lived loop sources raised by Ryan & de Nolfo (2018). However, the challenges for their model are: to describe where the proposed loops are located relative to the CMEs, what their observable signatures would be in X-ray or EUV coronal images, and how they maintain their closed magnetic integrities throughout the eruptive events. If turbulence is the acceleration mechanism, then we still confront the fundamental problem of maintaining a turbulent level in the loop large enough to accelerate $E \gtrsim 300$ MeV protons over many hours, as discussed in detail by Ryan (2000). The large-scale (up to several R_{\odot}) loops envisioned by Ryan & de Nolfo (2018) would likely be too weak to survive the disruption of a nearby fast and wide CME. If interchange reconnection is required to transport SEPs from open field lines to closed field loops (Hudson 2018), then the reconnection should have been manifested in the 1600 Å image brightenings of the Kazachenko et al. (2017) catalog. Because the SGRE events of Table 1 are located within 45° of the central meridian, any alleged loop footpoints containing the SEP precipitation should have been detected in the observations of enhanced 1600 Å emission, but we found that those emissions were limited to only the ARs and times of Table 1.

An attractive numerical model for accelerating SEPs to several hundred MeV on closed field lines of streamers has been discussed by Kong et al. (2017). In the streamer high-energy particles are more efficiently accelerated due to perpendicular shock geometry and the trapping effect of closed fields, with maximum acceleration at the top of closed magnetic field lines. This model achieves both the high particle

energies and loop trapping of the Hudson (2018) and Ryan & de Nolfo (2018) scenarios, but it constitutes a passive trapping model for which a very low level of turbulent pitch-angle scattering is required to maintain the hours-long trapping times (Hudson & Ryan 1995). At root, however, it is also a variant of the CME-driven shock model in which protons are accelerated on closed as well as open field lines. No additional acceleration or trapping mechanisms are required, although the helmet part of an energetic-proton-populated helmet streamer might constitute a quasi-stable loop in the Ryan & de Nolfo (2018) picture.

Additional observational and modeling evidence for the shock-precipitation picture has been published recently. Omodei et al. (2018) analyzed LAT observations of the 2017 September 10 GLE-associated flare for which >100 MeV emission lasted for >12 hr, beginning during the flare impulsive phase. From a timing comparison of the >100 MeV emission and the GLE, they infer that the post-flare component of the SGRE originated in a CME-driven shock wave. Winter et al. (2018) compared SGREs, encompassing observations from *SMM* through *Fermi*, with SEPs in space, taking soft X-ray flare and CME observations into account. Following Ryan (2000), they used the term long-duration gamma-ray flares, or LDGRFs. Their preliminary association analyses favored the proton precipitation scenario, although with a prominent counter-example on 2011 March 7.

Gopalswamy et al. (2018) found close matches between durations and ending times of 13 SGRE events and their associated interplanetary type II radio bursts, suggesting that the electrons producing type II shocks and the protons producing SGRE events are accelerated in the same shocks. They suggested that the lack of $E > 300$ MeV protons observed at 1 au during the 2011 March 7 SEP event and SGRE was due to its poor solar latitudinal magnetic connectivity. The low energy and delayed SEP injection of that event were cited by Winter et al. (2018) as an unexplained exception to and by Klein et al. (2018) as good evidence against the shock-source concept for SGREs. Both Gopalswamy et al. (2018) and Winter et al. (2018) found close connections between SGREs and very fast ($\nu > 2000$ km s $^{-1}$) and wide CMEs, again consistent with the shock-source scenario. This association of SGREs with fast CMEs raises the question for the posited quasi-stable loop picture of Ryan & de Nolfo (2018) of why SGREs are not observed in association with the more frequently occurring slower (less-energetic) CMEs that would be expected to disturb—and excite turbulence in—nearby helmet streamers without disrupting them.

Jin et al. (2018) simulated the CME-driven shock in the behind-the-limb long-duration LAT event of 2014 September 1, focusing on the magnetic connection between the shock and the >100 MeV front-side emission region. Their dynamic simulation showed: (1) magnetic connection between the shock and a visible disk coronal hole (as well as between the shock and the occulted flare site), and (2) a drop-off in intensity of the *Fermi*/LAT >100 MeV emission during the time that the shock geometry began changing from quasi-perpendicular to quasi-parallel. As Jin et al. (2018) note, these findings provide strong support for the shock-precipitation hypothesis for the sustained gamma-ray emission in this event.

4. Summary

We have compared the times of magnetic reconnection in AR flare ribbons with those of 11 associated SGRE events of the survey of Share et al. (2018). The SGRE events continue typically for hours after the reconnection episodes have concluded, showing that the reconnected loop structures provide neither an energy source for high-energy SEP production nor a trapping process for SEPs produced elsewhere in the corona. The result favors the concept of precipitation back to the Sun from a fraction of shock-accelerated SEPs over the alternative loop-trapping scenario for SGRE events.

S. Kahler was funded by AFOSR Task 18RVCOR122. We thank the reviewer for their helpful suggestions and comments, which improved the manuscript.

ORCID iDs

S. W. Kahler  <https://orcid.org/0000-0002-0470-7236>
 E. W. Cliver  <https://orcid.org/0000-0002-4342-6728>
 M. Kazachenko  <https://orcid.org/0000-0001-8975-7605>

References

- Ackermann, M., Ajello, M., Albert, A., & Allafort, A. 2014, *ApJ*, **787**, 15
 Ackermann, M., Allafort, A., Baldini, L., Barbiellini, G., et al. 2017, *ApJ*, **835**, 219
 Afanasiev, A., Aran, A., Vainio, R., et al. 2018, *ASSL*, **444**, 157
 Ajello, M., Albert, A., Allafort, A., Baldini, L., et al. 2014, *ApJ*, **789**, 20
 Akimov, V. V., Ambrož, P., Belov, A. V., Berlicki, A., et al. 1996, *SoPh*, **166**, 107
 Atwood, W. B., Abdo, A. A., Ackermann, M., Althouse, W., et al. 2009, *ApJ*, **697**, 1071
 Cliver, E. W., Kahler, S. W., Kazachenko, M., & Shimojo, N. 2018, *ApJ*, submitted
 Cliver, E. W., Kahler, S. W., & Vestrand, W. T. 1993, *Proc. ICRC (Tsukuba)*, **3**, 91
 Forrest, D. J., Vestrand, W. T., Chupp, E. L., Rieger, E., et al. 1985, *Proc. ICRC*, **4**, 146
 Gopalswamy, N., Mäkelä, P., Yashiro, S., Lara, A., et al. 2018, *ApJL*, in press
 Hudson, H., & Ryan, J. 1995, *ARA&A*, **33**, 239
 Hudson, H. S. 2018, in *IAU Symp. 335, Space Weather of the Heliosphere: Processes and Forecasts*, ed. C. Foullon & O. Malandraki (Cambridge: Cambridge Univ. Press), 49
 Jin, M., Petrosian, V., Liu, W., Nitta, N. V., et al. 2018, *ApJ*, submitted
 Kahler, S. W., Kazachenko, M., Lynch, B. J., & Welsch, B. T. 2017, *J. Phys. Conf. Ser.*, **900**, 012011
 Kanbach, G., Bertsch, D. L., Fichtel, C. E., Hartman, R. C., et al. 1993, *A&AS*, **97**, 349
 Kazachenko, M. D., Lynch, B. J., Welsch, B. T., & Sun, X. 2017, *ApJ*, **845**, 49
 Klein, K.-L., Tziotziou, K., Zucca, P., et al. 2018, *ASSL*, **444**, 133
 Kocharov, L., Laitinen, T., Vainio, R., et al. 2015, *ApJ*, **806**, 80
 Kong, X., Guo, F., Giacalone, J., Li, H., et al. 2017, *ApJ*, **851**, 38
 Kuznetsov, S. N., Kurt, V. G., Yushkov, B. Y., Myagkova, I. N., et al. 2014, *ASSL*, **400**, 301
 Mandzhavidze, N., & Ramaty, R. 1992, *ApJ*, **396**, L111
 Murphy, R. J., Dermer, C. D., & Ramaty, R. 1987, *ApJS*, **63**, 721
 Omodei, N., Pesce-Rollins, M., Longo, F., Allafort, A., et al. 2018, *ApJL*, submitted
 Pesce-Rollins, M., Omodei, N., Petrosian, V., Liu, W., et al. 2015, *ApJL*, **805**, L15
 Plotnikov, I., Rouillard, A. P., & Share, G. H. 2017, *A&A*, **608**, A43
 Qiu, J., Liu, C., Gary, D. E., Nita, G. M., & Wang, H. 2004, *ApJ*, **612**, 530
 Ramaty, R., & Mandzhavidze, N. 1996, in *AIP Conf. Proc. 374, High Energy Solar Physics*, ed. R. Ramaty et al. (Melville, NY: AIP), 533
 Ramaty, R., Murphy, R. J., & Dermer, C. D. 1987, *ApJL*, **316**, L41
 Ryan, J. M. 2000, *SSRv*, **93**, 581
 Ryan, J. M., & de Nolfo, G. A. 2018, in *Proc. Triennial Earth-Sun Summit Conf. (Washington, DC: AGU)*, 219.06
 Share, G. H., Murphy, R. J., Tolbert, A. K., Dennis, B. R., et al. 2018, *ApJS*, in press
 Sheeley, N. R., Jr., & Wang, Y.-M. 2014, *ApJ*, **797**, 10
 Toriumi, S., Schrijver, C. J., Harra, L. K., et al. 2017, *ApJ*, **834**, 56
 Vestrand, W. T., & Forrest, D. J. 1993, *ApJL*, **409**, L69
 Winter, L. M., Bernstein, V., Omodei, N., & Pesce-Rollins, M. 2018, *ApJ*, **864**, 39